A New High Step-Up DC-DC Converter for Renewable Energy Applications

Anh-Vu Ho[1(✉)], Thanh-Son Nguyen[1], Duc-Linh Tran[2], and Hoai-Nghia Duong[1]

[1] School of Engineering, Eastern International University, Thủ Dầu Một, Binh Duong, Vietnam
{vu.ho, son.nguyen, nghia.duong}@eiu.edu.vn
[2] School of Engineering, RMIT University, Melbourne, Australia
s3358328@student.rmit.edu.au

Abstract. This paper presents a new non-isolated boost converter with high boost ability and low voltage stress on the main switch. The proposed converter uses a hybrid switched-inductor (SL)/switched-capacitor (SC) technique to couple with an active switched network. The proposed converter is very suitable for many industrial applications such as photovoltaic (PV) and fuel-cell. A multicell hybrid SL/SC structure of the proposed converter is also derived in order to get a higher boost ratio. The operation principle, parameter design, and comparison with other converters are given. A laboratory prototype with the closed-loop control is designed for test, and both simulation and experimental results are given to demonstrate the effectiveness of the proposed converter.

Keywords: DC/DC converter · High step-up voltage ratio · Switched-capacitor Switched-inductor

1 Introduction

Nowadays, renewable energy resources such as fuel-cell, wind, photovoltaic (PV) systems have been significantly increased due to the impact of energy crisis and environmental pollution. In the renewable energy generation systems, a conventional boost converter is normally used for boosting voltage [1–3]. Theoretically, the boost converter can generate an infinite voltage gain when the duty ratio will tend to 1. However, the voltage gain of the boost inverter can maximally operate in 5–6 times of the input voltage in practical applications because the effects of on diodes, switches, and parasitic components of capacitors and inductors [4–6].

In order to increase the boost ability and the conversion efficiency, many high boost converter topologies have been introduced. The cascade boost converter can reach the requirements of the renewable energy resources applications [7, 8]. Although these converters have relatively high efficiency, but the complex combination and high components will be the major drawbacks of them. Recently, the switched-capacitor (SC), switched-inductor (SL), hybrid SC/SL techniques are used to achieve high step-up voltage gain [9, 10]. A non-isolated boost converter with multi-cell SC is proposed in [11]. Its advantages are transformer-less high conversion gain and modular

Y. Chen and T. Q. Duong (Eds.): INISCOM 2017, LNICST 221, pp. 307–318, 2018.
https://doi.org/10.1007/978-3-319-74176-5_27

structure. However, the use of SC technique will cause a high surge current. Based on the coupled inductor technique, several boost converters in [12–14] can improve boost capability and reduce the sizes. Their conversion efficiency is, however, reduced because the losses associated with leakage inductors. In addition, these topologies sustain a high voltage rated switch and suffer from electromagnetic interference (EMC). Single switch isolated boost converters using magnetic coupling such as fly-back converter or single-ended primary inductance converter (SEPIC) are proposed in [15, 16]. In fact, these converters can easily reach a high boost gain by increasing the turn ratio of the transformer. However, the leakage inductance of the transformer and voltage spike are inevitable and the voltage stress on the main switch will be increased. In [17], a 3-Z-network boost converter including three active Z-networks is presented to achieve high voltage gain. But its voltage gain may be still not enough for many applications that needs a stronger voltage gain. Additionally, a large number of diodes are used for the Z-network, they will reduce the conversion efficiency with an extremely high duty cycle. Some voltage lift techniques are proposed in [18, 19]. A high boost factor can be obtained by the transferred energy from the intermediate capacitor, but both capacitor voltage stress and current stress are significantly increased. A combination of SL/SC technique in [9] and active network [20] is proposed in [21, 22]. These converters not only extend the voltage gain but also reduce the voltage stress on the switching device. However, these converters contain high voltage stress on the main switching and high conduction loss.

In this paper, a new non-isolated boost converter with high boost ability and low voltage stress on the main switch is proposed. The proposed converter uses a hybrid SC/SL technique to couple with an active switched network. In this topology, a symmetrical impedance structure is employed and two switches control the same gating signal. The proposed converter is very suitable in applying to low input voltage of PV or fuel-cells. The operation principle, steady state analysis, and comparison with different ASN boost converters are given. A 100 W laboratory prototype is designed for test. Both simulation and experimental results are given to demonstrate the effectiveness of the proposed converter.

Main applications of the proposed converter will be in the renewable energy systems such as the PV or Fuel-cell applications. A typical application of the proposed converter in the PV distributed system is presented in Fig. 1. In this system, the output voltage of solar panels is often low dc voltage and uncontrollability due to the influences of environment, so the dc output voltage must be boosted and regulated via a step-up stage. Then, a desired output voltage is obtained and connected to a dc load or utility grid connected inverter.

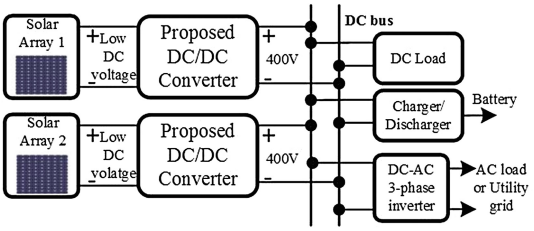

Fig. 1. Typical application of the proposed converter in PV distributed system

2 Review of Active-Switched Network Boost Converters

In this study, the existed active-switched network ASN boost converters topologies are reviewed and analyzed. Figure 2 shows the basic ASN boost converter [20] and SC-ASN boost converter [21].

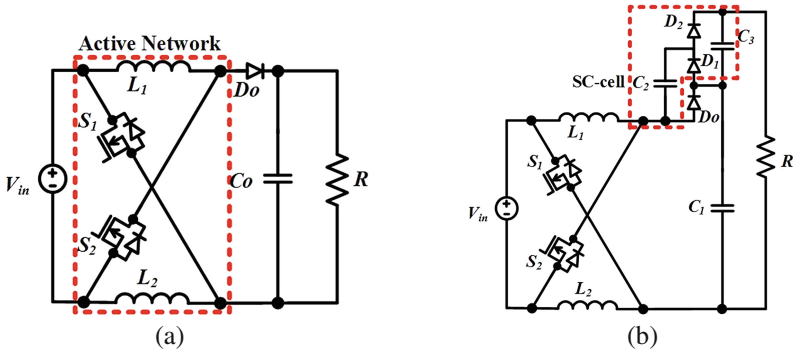

Fig. 2. Active-switched network converter: (a) ASN boost converter, (b) SC-ASN converter

The ASN boost converter concludes two inductors (L_1, L_2) with the same inductance value and two active switches (S_1, S_2) with the same gating signal as shown in Fig. 2(a). During the on-state of the switches, two inductors are charged by the input source and during the off-state, two inductors are delivered energy to the load.

The boost factor of the ASN boost converter is defined as follows

$$B = \frac{1+D}{1-D} \tag{1}$$

The SC-ASN boost converter is shown in Fig. 2(b) with a high boost factor. In this converter, the C_2 capacitor is charged while C_1 and C_3 are discharged during the switches are turned on. During the off-state, C_1 and C_3 are charged whereas C_3 is discharged. The boost factor of the SC-ASN converter is be calculated as

$$B = \frac{3+D}{1-D} \tag{2}$$

Figure 3 shows two kinds of the improved ASN boost converter. The Fig. 3(a) proposes the SL-ASN boost converter with a symmetrical structure [21, 22]. In this topology, four inductors are charged by the input source during the on-state of the switches and discharged to the load during the off-state of the switches. In the SL-cell, two inductor is in series during the on-state of switches and in parallel during the off-state of switches. The boost factor of the SL-ASN converter can be calculated as follows

$$B = \frac{1+3D}{1-D} \tag{3}$$

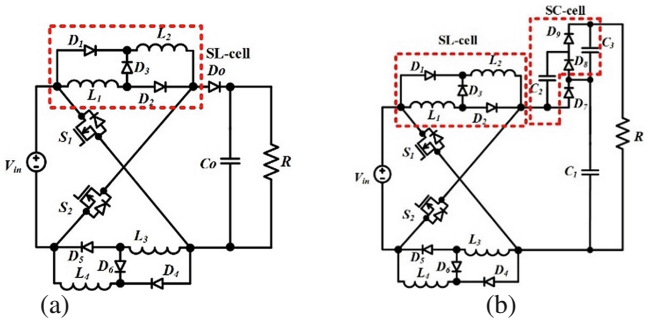

Fig. 3. Improved ASN boost converters: (a) SL-ASN converter and (b) SC/SL-ASN converter

The SC/SL-ASN converter is shown in the Fig. 3(b). The higher boost factor can be achieved with both SL and SC technique. The boost factor of the SL/SC ASN boost converter can be expressed as

$$B = \frac{3 + 5D}{1 - D} \tag{4}$$

3 Operating Principle of the Proposed Converter

In the Fig. 4, the proposed hybrid SC/SL-ASN converter based on the ASN converter is proposed. It is a combination between the active switched network and two hybrid SC/SL-cells. The switching action of the switches will be changed the connection of the hybrid SC/SL-cells.

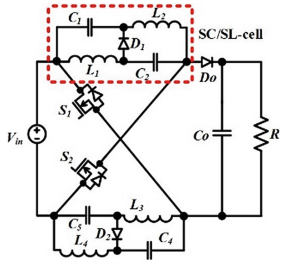

Fig. 4. SC/SL-ASN boost converter

The operating principles in continuous-conduction mode (CCM) of the proposed converter will be discussed in this section. Figure 5 illustrates the operating modes during one switching period and the theoretical waveforms for one switching cycle are given in Fig. 6. For simplicity the analysis of the operating principles, the following assumptions are considered: (1) the capacitors of the proposed converter is large enough so that the voltage on them are assumed to be constant. (2) the switches and diodes are ideal components.

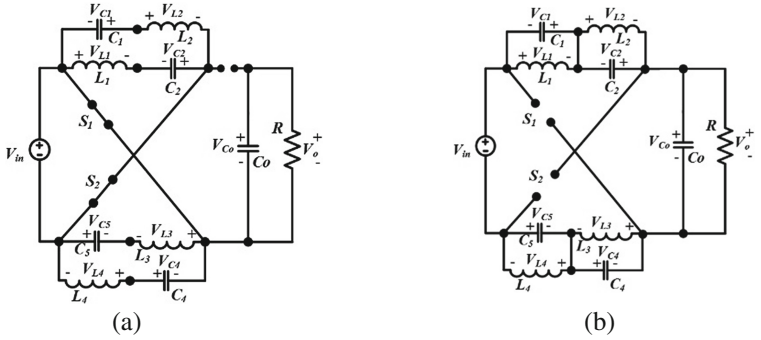

Fig. 5. Operating states of the proposed SC/SL-ASN boost converter in CCM. (a) Mode 1 ($t_0 - t_1$). (b) Mode 2 ($t_1 - t_2$).

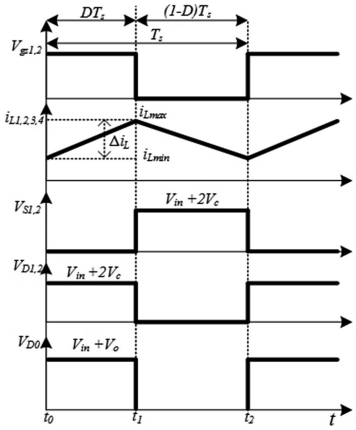

Fig. 6. Theoretical waveforms of the proposed SC/SL-ASN boost converter in CCM

(1) In mode 1 [$t_0 - t_1$]. During this interval, two switches S_1 and S_2 are turned on, while diodes D_1, D_2, and D_0 are reverse biased. The equivalent circuit is shown in Fig. 5(a). Four inductors L_1, L_2, L_3 and L_4 are charged by C_1, C_2, C_3 and C_4, respectively. The capacitor C_0 is delivered to the load.

Because the symmetrical characteristic of this converter ($C_1 = C_2 = C_3 = C_4$ and $L_1 = L_2 = L_3 = L_4$). The following equations can be given as

$$v_{L1} = v_{L2} = v_{L3} = v_{L4} \text{ and } V_{C1} = V_{C2} = V_{C3} = V_{C4} \tag{5}$$

Based on the KVL, we have

$$v_{L1} = V_{C2} + V_{in} \tag{6}$$

(2) In mode 2 [$t_1 - t_2$]. During this interval, two switches S_1 and S_2 are turned off, while diodes D_1, D_2, and D_0 are forward biased. The equivalent circuit is shown in

Fig. 5(b). Four inductors L_1, L_2, L_3 and L_4 are released the energy to the capacitor C_0 and the load.

Based on the KVL, the following equations can be derived as

$$v_{L1} = -V_{C1} = \frac{V_{in} - V_o}{4} \tag{7}$$

$$V_o = V_{in} + V_{C1} + V_{C2} + V_{C3} + V_{C4} \tag{8}$$

By applying the voltage-second balance principle to the inductor L_1, the following relationships can be obtained.

$$V_{C1} = V_{C2} = V_{C3} = V_{C4} = \frac{1}{1-2D} V_{in} \tag{9}$$

$$V_o = \frac{1+2D}{1-2D} V_{in} \tag{10}$$

From (10), the voltage gain B of the proposed converter is given as

$$B = \frac{V_o}{V_{in}} = \frac{1+2D}{1-2D} \tag{11}$$

4 Performance Comparisons with Different ASN Converters

In this section, the performances of the proposed converter and the existing boost converter topologies are compared. We assume that all converters are operated with the same condition.

Comparison of the number of components used in the proposed converter and different ASN boost converters are presented in Table 1. From this table, all the converters used two active switches. In compared with the SC/SL-ASN converter, the proposed converter used lower six diodes and more two capacitors. But, the voltage gain is stronger than that of the SC/SL ASN converter.

Table 1. Performance comparison with different ASN converters

Converters	Proposed	SC/SL-ASN	SC-ASN	SL-ASN
Inductor	4	4	2	4
Capacitors	5	3	3	1
Diodes	3	9	3	7
Switches	2	2	2	2
Voltage gain	$\frac{1+2D}{1-2D}$	$\frac{3+5D}{1-D}$	$\frac{3+D}{1-D}$	$\frac{1+3D}{1-D}$
Voltage stress	$\frac{2(B+1)}{B+3}$	$\frac{5+B}{8}$	$\frac{B+1}{4}$	$\frac{B+3}{4}$

As shown in Fig. 8, it is seen that the voltage gain of the proposed converter is higher than that of the other converters when the duty cycle is higher than 0.4. In an example, a fifteen times voltage gain of the proposed converter can be obtained at D = 0.43 while the voltage gain of the SC/SL-ASN converter is only nine times. Thus, the proposed converter can significantly reduce the current ripple and volume of the converters (Fig. 7).

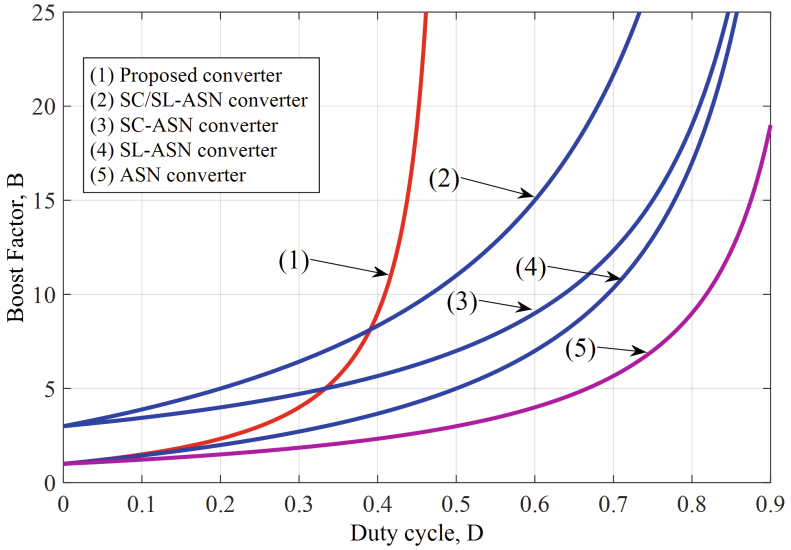

Fig. 7. Comparison of boost capability between different converters

The relationship between the normalized voltage stresses across the main switches of the proposed converter shows in Fig. 9. According to this figure, the voltage stress on the main switch of the proposed converter is lower than that of the other ASN boost converters. It means that a lower rating of the main switches can be used, which will reduce the cost and improve the efficient of the converters.

5 Simulation and Experimental Results

5.1 Simulation Results

In order to verify the performances of the proposed converter, the simulations in PSIM program based on the open loop control are presented. The circuit parameters used for the simulation is shown in Table 2.

The simulation results of the proposed converter are presented in Fig. 10. From this figure, it can be seen that the converter operates in CCM. Figure 9(a) shows the output voltage is boosted to 60 V when the duty cycle D = 0.3 and the input voltage V_{in} = 15 V. The current inductors linearly increased during the switches are turned on and linearly

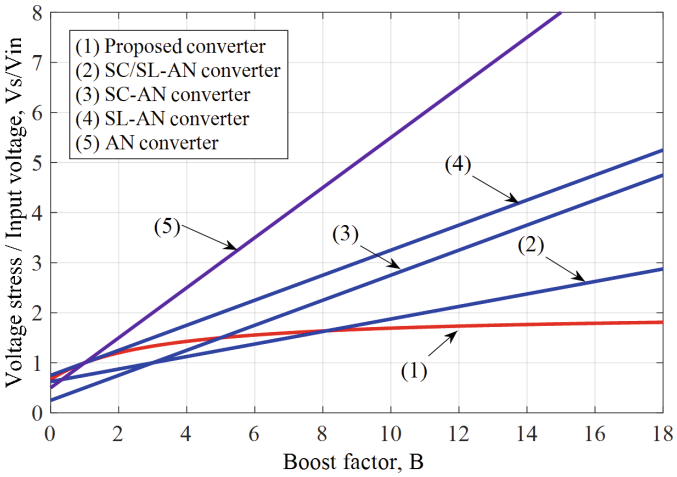

Fig. 8. Comparison of voltage stress between different converters

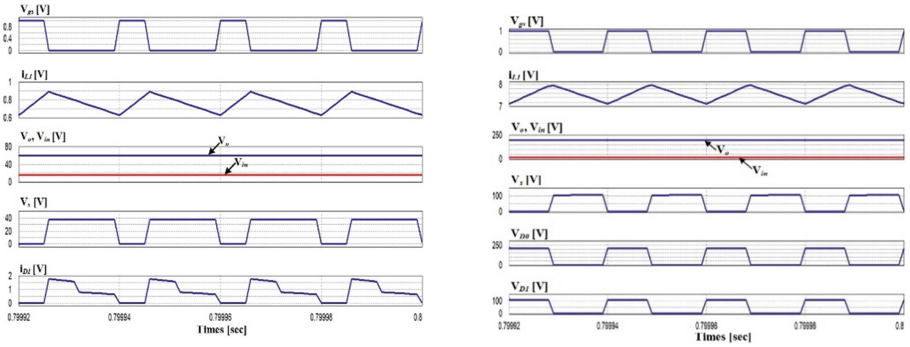

(a) (b)

Fig. 9. Simulation results when V_{in} = 15 V: (a) D = 0.3, (b) D = 0.42

Table 2. Parameters used in simulation and experiment

Parameter	Symbol	Value
Input voltage	V_{in}	15 V
Output voltage	V_o	200 V
Maximum output voltage	P_o	100 W
Switching frequency	f_s	50 kHz
Inductors	L_1, L_2, L_3, L_4	0.6 mH
Capacitors	C_1, C_2, C_3, C_4	100 µF/50 V
Output capacitor	C_o	500 µF/250 V

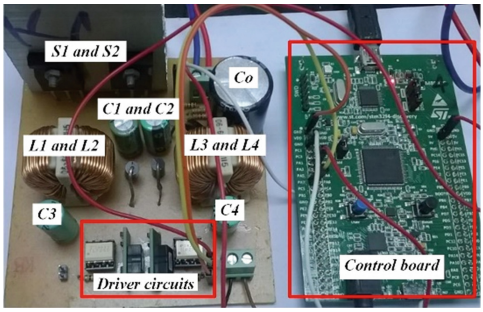

Fig. 10. Photograph of the experimental prototype.

decrease during the switches are turned off. When the duty cycle is increased to 0.42, the output voltage is boosted to 200 V. These simulation results are similar to the theoretical calculations.

5.2 Experimental Results

A 100 W experimental prototype of the proposed converter, as shown in Fig. 10, has been built in the laboratory to verify the theoretical analysis and to validate the simulation results. The experimental parameters are used the same as the circuit parameters in Table 1. The control board is based on the 32-bit STM32F407VGT6 microcontroller.

Figure 11 shows the experimental results of the proposed converter under different conditions. In the Fig. 10(a), the experimental waveforms of the proposed converter under the condition V_{in} = 15 V and D = 0.2, the measured value of the output voltage is 37.4 V. Figure 10(b) shows the experimental result when the duty cycle is increased to 0.3, the measured value of the output voltage is 55 V, which is lower than the theoretical value is 60 V.

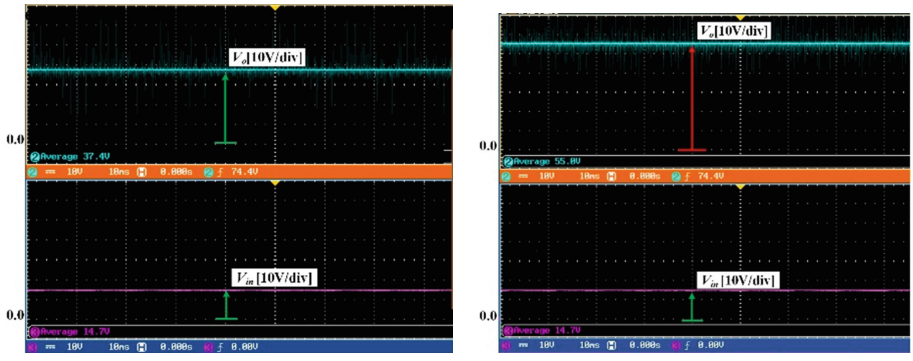

(a) (b)

Fig. 11. Experimental results when V_{in} = 15 V: (a) D = 0.2 and (b) D = 0.3

The performance of the proposed converter is investigated to confirm the transient response of the output voltage under the condition of duty cycle changes from 0.2 to 0.3. It can be observed in the Fig. 12 that the variation in the output voltage is jumped from 37 V to 55 V while the input voltage is kept at 15 V.

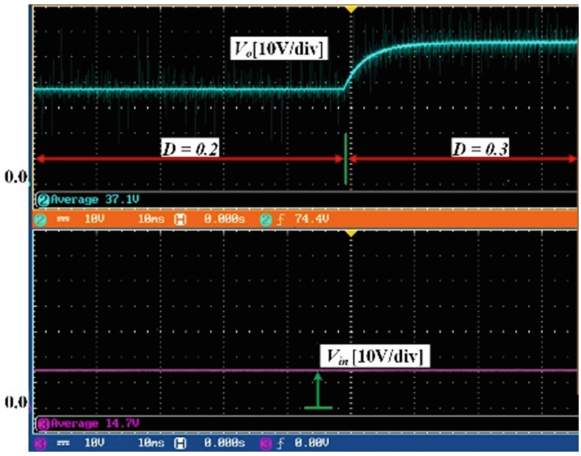

Fig. 12. Experimental results in transient response when duty cycle changes from 0.2 to 0.3

Figure 13 represents a comparison of the experimental and theoretical boost factor of the proposed converter when V_{in} = 15 V and f_s = 50 kHz. It is clearly seen that the experimental values are agreement with the theoretical values when taking into account the effectivity of the parasitic components on the inductors and capacitors as well as the forward voltage drop of the diodes. The differences between the calculated values and the experimental values are an increasing trend as the use of a higher duty cycle.

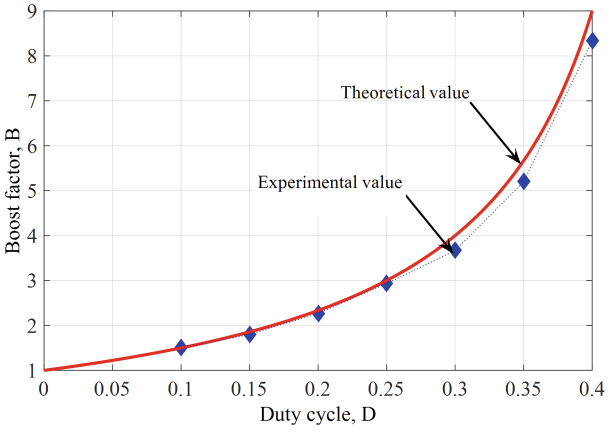

Fig. 13. DC voltage gain of the proposed converter

6 Conclusions

In this paper, a high boost capability converter is introduced to the renewable energy systems such as PV systems. The proposed converter uses two active switches and a symmetrical structure with two hybrid switched-capacitor/switched-inductor cells. The proposed converter can obtain a high voltage gain, with transformerless conversion, and also sustain low voltage stress across all main switches. Operation principles and its features have been discussed in the paper. Comparisons between the proposed converter and the existing active switches boost converters, the proposed converter has a higher voltage gain for $D \geq 0.4$ as well as a lower voltage stress across the active switches, which requires a lower-voltage-rated MOSFET switch with a smaller drain-to-source resistance and can use Schottky diodes to reduce the reverse-recovery current problem. Thus, the proposed converter can be a competitive alternative for real applications where a high voltage capability is required. Finally, both simulations and experimental results are carried out to verify the functionality and the theoretical analysis.

References

1. Blaabjerg, F., Yang, Y., Ma, K.: Power electronics - key technology for renewable energy systems - status and future. In: 2013 3rd International Conference on Electric Power and Energy Conversion Systems, pp. 1–6 (2013)
2. Samavatian, V., Radan, A.: A high efficiency input/output magnetically coupled interleaved buck-boost converter with low internal oscillation for fuel-cell applications: CCM steady-state analysis. IEEE Trans. Industr. Electron. **62**, 5560–5568 (2015)
3. Zhu, H., Zhang, D., Athab, H.S., Wu, B., Gu, Y.: PV isolated three-port converter and energy-balancing control method for PV-Battery power supply applications. IEEE Trans. Industr. Electron. **62**, 3595–3606 (2015)
4. Ismail, E.H., Al-Saffar, M.A., Sabzali, A.J., Fardoun, A.A.: A family of single-switch PWM converters with high step-up conversion ratio. IEEE Trans. Circuits Syst. I Regul. Pap. **55**, 1159–1171 (2008)
5. Choi, H., Ciobotaru, M., Jang, M., Agelidis, V.G.: Performance of medium-voltage DC-Bus PV system architecture utilizing high-gain DC-DC converter. IEEE Trans. Sustain. Energ. **6**, 464–473 (2015)
6. Tsai, J.C., Chen, C.L., Lee, Y.H., Yang, H.Y., Hsu, M.S., Chen, K.H.: Modified hysteretic current control (MHCC) for improving transient response of boost converter. IEEE Trans. Circuits Syst. I Regul. Pap. **58**, 1967–1979 (2011)
7. Matsuo, H., Harada, K.: The cascade connection of switching regulators. IEEE Trans. Ind. Appl. **IA-12**, 192–198 (1976)
8. Xiong, S., Tan, S.C.: Cascaded high-voltage-gain bidirectional switched-capacitor DC-DC converters for distributed energy resources applications. IEEE Trans. Power Electron. **32**, 1220–1231 (2017)
9. Axelrod, B., Berkovich, Y., Ioinovici, A.: Switched-capacitor/switched-inductor structures for getting transformerless hybrid DC-DC PWM converters. IEEE Trans. Circuits Syst. I Regul. Pap. **55**, 687–696 (2008)

10. Tan, S.C., Nur, M., Kiratipongvoot, S., Bronstein, S., Lai, Y.M., Tse, C.K., Ioinovici, A.: Switched-capacitor converter configuration with low EMI emission obtained by interleaving and its large-signal modeling. In: 2009 IEEE International Symposium on Circuits and Systems, pp. 1081–1084 (2009)
11. Ganesan, R.G., Prabhakar, M.: Non-isolated high gain boost converter for photovoltaic applications. In: 2013 International Conference on Power, Energy and Control (ICPEC), pp. 277–280 (2013)
12. Hsieh, Y.P., Chen, J.F., Yang, L.S., Wu, C.Y., Liu, W.S.: High-conversion-ratio bidirectional DC-DC converter with coupled inductor. IEEE Trans. Industr. Electron. **61**, 210–222 (2014)
13. Freitas, A.A.A., Tofoli, F.L., Júnior, E.M.S., Daher, S., Antunes, F.L.M.: High-voltage gain DC-DC boost converter with coupled inductors for photovoltaic systems. IET Power Electron. **8**, 1885–1892 (2015)
14. Tang, Y., Fu, D., Wang, T., Xu, Z.: Analysis of active-network converter with coupled inductors. IEEE Trans. Power Electron. **30**, 4874–4882 (2015)
15. Kwok-Wai, M., Yim-Shu, L.: An integrated flyback converter for DC uninterruptible power supply. IEEE Trans. Power Electron. **11**, 318–327 (1996)
16. Gules, R., Santos, W.M.D., Reis, F.A.D., Romaneli, E.F.R., Badin, A.A.: A modified SEPIC converter with high static gain for renewable applications. IEEE Trans. Power Electron. **29**, 5860–5871 (2014)
17. Zhang, G., Zhang, B., Li, Z., Qiu, D., Yang, L., Halang, W.A.: A 3-Z-Network boost converter. IEEE Trans. Industr. Electron. **62**, 278–288 (2015)
18. Luo, F.L.: Positive output Luo converters: voltage lift technique. IEE Proc. Electr. Power Appl. **146**, 415–432 (1999)
19. Jiao, Y., Luo, F.L., Zhu, M.: Voltage-lift-type switched-inductor cells for enhancing DC-DC boost ability: principles and integrations in Luo converter. IET Power Electron. **4**, 131–142 (2011)
20. Yang, L.S., Liang, T.J., Chen, J.F.: Transformerless DC-DC converters with high step-up voltage gain. IEEE Trans. Industr. Electron. **56**, 3144–3152 (2009)
21. Tang, Y., Wang, T., Fu, D.: Multicell switched-inductor/switched-capacitor combined active-network converters. IEEE Trans. Power Electron. **30**, 2063–2072 (2015)
22. Tang, Y., Fu, D., Wang, T., Xu, Z.: Hybrid switched-inductor converters for high step-up conversion. IEEE Trans. Industr. Electron. **62**, 1480–1490 (2015)